

A Hybrid Level Set Based Approach for Surface Water Delineation using Landsat-8 Multispectral Images

Bijeesh TV, Narasimhamurthy KN

Abstract—The detection and delineation of surface water is a crucial step in change detection studies on water bodies using satellite images. Single band methods, spectral index methods, classification using machine learning and spectral un-mixing methods are the widely used strategies for surface water mapping from multi-spectral images. Level set theory based algorithms have been successfully employed in image segmentation problems and are proven to be effective. This study presents a hybrid level set theory based segmentation algorithm which is a combination of edge based and region based approaches to detect and delineate surface water bodies in Landsat 8 images. Level set algorithms were applied in combination with Modified Normalized Difference Water Index (MNDWI) to further improve the delineation accuracy. Robustness of the proposed approach was established by successfully applying the algorithm to delineate water bodies of different sizes, ranging from 0.5 km² to 298 km² in surface area. The proposed algorithm was also compared with established machine learning based delineation methods and found to be faster than the algorithms those produced comparable delineation outputs. As the ground truth was not available for accuracy measurement, the output image of the proposed method was compared with the outputs of the machine learning algorithms using Pearsons correlation coefficient, Structural Similarity Index (SSIM) and Dice Similarity Index. The proposed algorithm was subsequently applied to multi-temporal Landsat data for water body change detection and analysis.

Index Terms—Level Sets, Landsat8 Multispectral Images, Modified Normalized Water Index, Surface Water Delineation

I. INTRODUCTION

WATER is one of the natural resources that is essential for the existence of life and needs to be conserved. Change detection studies on surface water bodies have been utmost important to researchers and administrators, as it can help in designing strategies to conserve them. Monitoring the temporal changes to the water bodies is a very time consuming and costly task. Researchers have been trying to develop semi-automated and automated systems to perform change detection with the help of satellite images available. With the advent of complex digital image processing algorithms, it is now possible to develop fully automated systems for change detection. Multispectral and hyperspectral images captured by satellites are now available to the research community at various open on-line portals. By using suitable image processing algorithms, the

otherwise concealed insights in these multi-spectral data can be extricated and studied to better understand the natural resource under study.

Multi-spectral imagery is an advanced form of optical imaging in which multiple monochrome images are captured together at different wavelength regions of the electro-magnetic spectrum. A multi-spectral image captures the wavelength and frequency information of each EM waves reflected/emitted from an object. This frequency information is useful in detecting and mapping different objects on earth's surface and also beneath the surface. Spectral imaging has its roots in spectroscopy which is the discipline of science studying the wavelength variations in light energy reflected or emitted from objects on the earth's surface in relation to wavelength. By juxtaposing images for various wavelengths, spectroscopy creates a data cube or a multi-spectral cube. Multi-spectral images are typically three-dimensional data cubes, (x, y, λ) , with x and y representing two spatial dimensions and λ representing the spectral dimension. Special sensors on satellites or specially built airborne spectrometers are typically used to capture such images. Multi-spectral remote sensing aims to observe, extract and analyze hidden and useful details from a given scene from its spectra. Such images can capture details that are otherwise undetectable to human eyes about a scene. Various objects on earth are found to exhibit unique spectral behavior which can be effectively utilized to detect and analyze the object under consideration. These spectral fingerprints are also referred to as spectral signatures. Since specific objects possess unique spectral signatures, these objects can be effectively observed and analyzed. Water has a distinct spectral signature in the Electro-Magnetic spectrum, which motivates the use of multi-spectral images for water body analysis. The vast majority of multi-spectral sensors collect images in the visible, near infrared, and infrared portions of the spectrum, making them ideal for water resource research.

Water body change monitoring is essential to analyze the long term and seasonal changes happening to water bodies. Accurate and automated water mapping is the key stage in performing such change monitoring. Most commonly used water delineation methods are spectral index based methods and machine learning based methods. This work proposes to develop a robust, automatic water delineation algorithm by employing a level set based algorithm on Landsat 8 multispectral images. A level set is an implicit representation of a curve. In level set based

Manuscript received October 20, 2020; revised Feb 04, 2021.

Bijeesh TV is a PhD scholar in the Department of Computer Science and Engineering, CHRIST (Deemed to be University), Bangalore. (E-mail : bijeesh.tv@christuniversity.in)

Narasimhamurthy KN is a professor in the Department of Civil Engineering, CHRIST (Deemed to be University), Bangalore. (E-mail : narasimha.murthy@christuniversity.in)

segmentation, we first arbitrarily fix our level set on the image and then evolve the level set according to some force. Though level set based segmentation has been used widely in many image processing applications, it has not been experimented adequately in remote sensing applications. Thomas Hahmann, Birgit Wessel developed semi-automated water body detection method using active contours on high resolution TerraSAR-X data [1]. Y.H. Dandawate and Sneha Kinlekar employed the modified Chan-Vese algorithm for rivers and coastline detection using Landsat 7 images [2]. An improved seeded region growing algorithm was developed by Jun Pan and Mi Wang for detection of water bodies from areal digital images [3]. A land surface water mapping method was developed by Chuan Xu, Haigang Sui and Feng Xu using visual saliency model and multi-scale level sets on SAR data [4]. Another level set based method was developed by Meng, Q, et. al. using the SAR data and factorization based active contours for water detection [5]. Zhang, Xiaokang, et al. used level sets incorporated with improved MRF to perform change detection in Landsat 7 images [6]. ZHANG Mei-mei, et.al. proposed an automated glacial lake mapping method using non-local active contours on Landsat 8 data [7].

Level set based method was effectively used for coastline detection from SAR images by researchers in the past. Modava and Akbarizadeh applied level set method in combination with fuzzy c-means clustering on the input SAR images to effectively detect the coastline. [13] [14] They have also developed coastline detection method by integrating spectral histogram and level sets. [15] This study proposes to develop an effective surface water delineation technique by applying a hybrid level set algorithm on Landsat 8 multispectral images which can further be used for automating change detection studies. The proposed algorithm takes into account the local and global image features to provide better segmentation results and appropriate preprocessing steps are presented which makes the algorithm robust and effective on multi-temporal data.

II. MATERIALS AND METHODS

A. Multispectral Data

Landsat 8 is the latest satellite to be launched collaboratively by National Aeronautics and Space Administration (NASA) and U.S.Geological Survey (USGS) in the Landsat series. Landsat satellites have a temporal resolution of 16 days; which means the image of a given scene is captured every 16 days. Landsat 8 has an Operational Land Imager (OLI) and a Thermal Infrared Sensor (TIRS) on board which are basically push broom instruments. A Landsat 8 multispectral image is made up of eleven electromagnetic bands each corresponding to a specific region in the electro-magnetic spectrum. It is composed of 9 sub-images that captures the frequency information and 2 sub-images that hold the temperature data. Every multi-spectral image is characterized by its spatial resolution apart from its temporal resolution. Landsat 8 data is acquired at thirty meters spatial resolution with the exception of PAN band. Band8 which is the panchromatic image has 15 meters resolution in the spatial dimension. In

the supplied product, the thermal bands those are originally captured at 100 meters spatial resolution, are up-sampled to 30 meters resolution. Table I presents the bandwidth and spatial resolution of all the Landsat 8 OLI bands. [11].

TABLE I: Landsat Multispectral Image Bands and details

| Landsat 5 | | | Landsat 8 | |
|-----------|--------------------------|---------------------|----------------------------|---------------------|
| Bands | Wavelength (micrometers) | Resolution (meters) | Wavelength (micrometers) | Resolution (meters) |
| B1 | Blue (0.45 - 0.52) | 30 | Ultra Blue (0.435 - 0.451) | 30 |
| B2 | Green (0.52 - 0.60) | 30 | Blue(0.452 - 0.512) | 30 |
| B3 | Red (0.63 - 0.69) | 30 | Green(0.533 - 0.590) | 30 |
| B4 | NIR (0.77 - 0.90) | 30 | Red(0.636 - 0.673) | 30 |
| B5 | SWIR1 (1.55 - 1.75) | 30 | NIR(0.851 - 0.879) | 30 |
| B6 | TIR (10.40 - 12.50) | 30 | SWIR1(1.566 - 1.651) | 30 |
| B7 | SWIR2 (2.09 - 2.35) | 30 | SWIR2(2.107 - 2.294) | 30 |
| B8 | Not Applicable | | PAN(0.503 - 0.676) | 15 |
| B9 | Not Applicable | | Cirrus(1.363 - 1.384) | 30 |
| B10 | Not Applicable | | TIRS1(10.60 - 11.19) | 100 * (30) |
| B11 | Not Applicable | | TIRS2(11.50 - 12.51) | 100 * (30) |

Band1 and Band9 were introduced as newer bands in Landsat 8 and can be used effectively for coastal and aerosol studies (Band1) and the detection of a common type of high altitude clouds called cirrus cloud (Band9). Band10 and Band11 are designed to be used in acquiring earth's surface temperature data more accurately than its predecessors. These two bands are thus called the thermal bands. The presence of Near Infrared (NIR) and Short Wave Infrared (SWIR) bands along with the visible bands makes Landsat 8 data ideal for remotely studying water resources as they have . NIR and SWIR bands are used successfully in most commonly used spectral water indices. Multispectral data from Landsat 8 are preferred by researchers as it consists of cirrus band that helps in observing and eliminating pixels corresponding to clouds in the scene effectively. Pansharpening is another widely used technique for enhancing a spectral band's spatial resolution by performing image fusion with a second image with higher spatial resolution. The spatial resolution of any Landsat 8 spectral band can be doubled by pansharpening it by using Panchromatic band (Band 8) that has double the resolution. Such pansharpened images with improved spatial resolution can be effectively utilized to obtain improved results while performing water delineation. All the Landsat data used and presented in this work are obtained from the USGS EROS portal as free downloads. EROS manages the Landsat project together with NASA and maintains an extensive archive of Earth's land surface satellite images. The water delineation algorithm proposed in this study is implemented using MATLAB 2016b running on a dual core intel processor. The complete flow diagram of the proposed hybrid level set based water delineation approach is presented in Figure 1.

B. Modified Normalized Difference Water Index (MNDWI)

Spectral indices are band ratios created by combining more than one spectral bands of hyperspectral or multispectral data. There are many proven spectral indices which are extensively used in surface water delineation. In this work, various spectral indices are evaluated for their usefulness to be used as a normalization stage in the water delineation algorithm. MNDWI combined with histogram equalization performs effectively as a normalization step in the proposed methodology. MNDWI is a simple spectral water index that

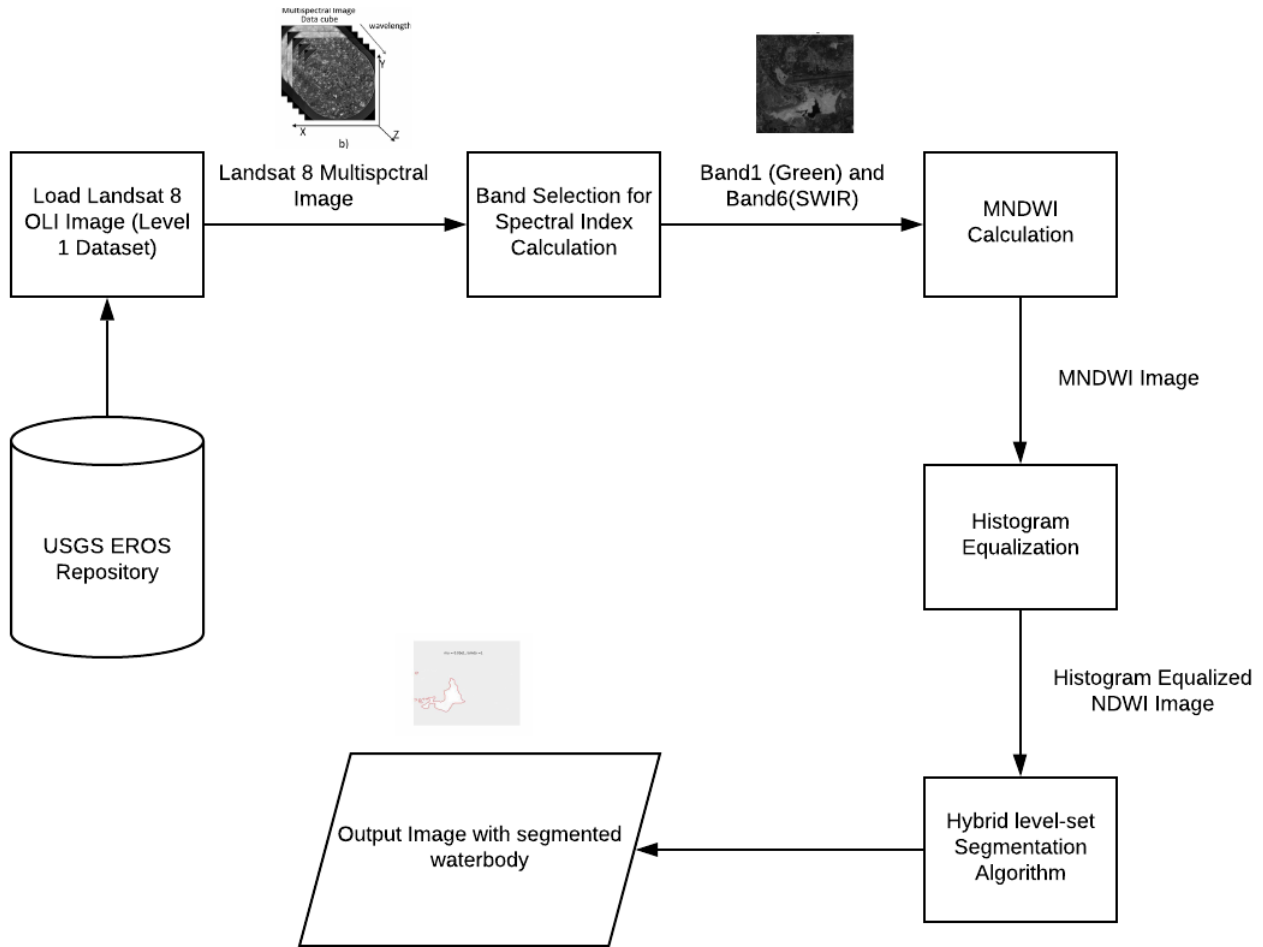


Fig. 1: Hybrid level set based Surface Water delineation methodology

uses the Green band and SWIR band of the Landsat 8 multispectral image and the formula to compute MNDWI is given in equation 1 [16]. The usefulness of MNDWI for water detection using Landsat 8 images was studied and presented in [12].

$$MNDWI = \frac{Green - SWIR}{Green + SWIR} \quad (1)$$

C. Level Set Theory

A level set is defined as an implicit representation of a curve. In level set based segmentation, we first arbitrarily fix our level set on the image and then evolve the level set according to some force [17] [18] [19]. Usually the force that controls the evolution of level set is the curvature of the corresponding level set function, which is a geometric property of the function. We use a special function called edge stopping function which stops the level set evolution at the image boundaries. Edge stopping function is usually a function of the image gradient. Level set based segmentation falls mainly into two categories: edge based segmentation and region based segmentation. Generally in a level set algorithm an initial level set function is chosen as an implicit representation of a curve. The initial level set also referred

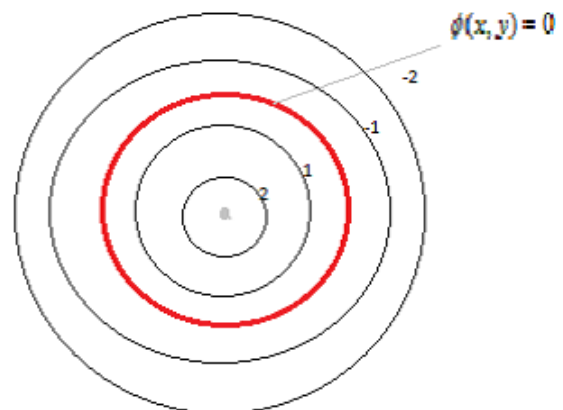


Fig. 2: Level set function

to as the initial contour C_0 is fixed randomly on the image domain and is evolved continuously based on a force function to finally stop based on a condition. Usually, a property of the image like image gradient is used as the level set evolution force.

Consider a level set function $\phi(x, y, t)$; where t is a time



Fig. 3: Level set evolution

variable introduced to evolve the level set with time. The continuous evolution of the level set curve is governed by equation 2.

$$\frac{\partial \phi}{\partial t} = F |\nabla \phi| \quad (2)$$

The function $\phi(x, y) = 0$ corresponds to the initial contour C_0 . The driving force F acts in a direction normal to the contour. Usually in a curve evolution model, the driving force F is the curvature of the level set curve, which is mathematically defined as given in equation 3.

$$F = \frac{\phi_y^2 \phi_{xx} - 2\phi_x \phi_y \phi_{xy} + \phi_x^2 \phi_{yy}}{(\phi_x^2 + \phi_y^2)^{3/2}} \quad (3)$$

$\nabla \phi$ is the gradient of the level set function $\phi(x, y, t)$.

This means that the level set evolution is controlled by two forces; the curvature of the function, which is a geometric quantity and the gradient of the level set function. The evolution continues until it can no longer evolve [20].

D. Image segmentation using level sets

One of the key applications of level sets is in image segmentation problems. Image segmentation is the process of detecting and separating out the regions of interest from the background in the image. To perform image segmentation using level set evolution method, we add a new term called edge stopping function the level set evolution PDE. So the new PDE is as shown in equation 4.

$$\frac{\partial \phi}{\partial t} = g(x, y) F |\nabla \phi| \quad (4)$$

Here the function $g(x, y) = \frac{1}{(1 + |\nabla f|^2)}$, where f is the image, is called the edge stopping function. The value of this function becomes nearly equal to zero at the object boundaries because of the fact that the image gradient is relatively higher at the boundaries. Therefore the edge stopping function becomes zero at the boundaries and thus the level set evolution stops at the image boundary. The level set evolution from initial contour to the final contour that fits the image boundaries is illustrated in Figure 3.

There are primarily two models for active contour based boundary detection, edge-based and region-based models. The former approach is typically based on the intensity shifts around an edge and can be formulated as function derivatives. Such methods employ the gradient of the image to build an edge stopping function which forces the contour evolution to stop at desired boundaries in the image. Nonetheless, the edge-based approach is not deemed the best because the edges may not be sharp due to ink fading or image deterioration which can prevent the gradient value at the edges from being a high value. Another disadvantage

of these models is that they are very much dependent on where the initial contour is placed within the image. Edge base models are said to have local segmentation property as they tend to properly segment the desired objects only if the initial level set is carefully placed around the region of interest.

Region-based model on the other hand does not work on the image discontinuity, but divides the image into objects and background based on similarity of pixel intensity. To control the evolution, region-based models use statistical information from pixels within and outside the contour. This makes it more noise-tolerant and gives improved segmentation accuracy on weak-edge and edge-free images. This approach is independent of the initial contour's location and scale and can effectively process interior and exterior boundaries simultaneously. Therefore region based models are said to possess global segmentation property.

The proposed work is built on a hybrid active contour segmentation model which exploits the benefits of edge and region based formulations to achieve better segmentation accuracy. The region based models try to find a global minimizer for the level set function while the edge bases models try to segment the image with respect to the local properties of the object. The proposed energy functional consists of terms corresponding to region based models and an edge stopping term that incorporates the local property of the image for segmentation. The final functional that needs to be minimized to achieve contour evolution leading to object segmentation is given in equation 5.

$$\begin{aligned} F(c_1, c_2, \phi) = & \mu \cdot \text{length}(\phi) \\ & + \lambda \int_{\text{inside}(C)} |u_0 - c_1|^2 dx dy \\ & + \lambda \int_{\text{outside}(C)} |u_0 - c_2|^2 dx dy \\ & + \int g(x, y) dx dy \end{aligned} \quad (5)$$

where c_1 and c_2 are the average pixel intensities of u_0 inside and outside the contour C respectively and μ , λ are weights. The length term is a regularization term and the subsequent two terms correspond to the region based energy and the last term is the edge stopping function. The term corresponding to the length of the level set curve be replaced with the corresponding integral and the we get equation 7.

$$\begin{aligned} F(c_1, c_2, \phi) = & \mu \int \delta(\phi(x, y)) |\nabla \phi(x, y)| dx dy \\ & + \lambda \int_{\text{inside}(C)} |u_0 - c_1|^2 dx dy \\ & + \lambda \int_{\text{outside}(C)} |u_0 - c_2|^2 dx dy \\ & + \int g(x, y) dx dy \end{aligned} \quad (6)$$

The function $\delta(\phi)$ is called the Dirac delta function of the Heaviside function H and it initializes the contour. Heaviside or unit step function is defined in equation 7 and the Dirac delta function is defined in equation 8.

$$H(z) = \begin{cases} 1, & \text{if } z \geq 0 \\ 0, & \text{if } z < 0 \end{cases} \quad (7)$$

$$\delta(z) = \frac{d}{dz} H(z) \quad (8)$$

In calculus, a function or a functional can be minimized by solving its equivalent Euler-Lagrangian formulation for the functional. The segmentation problem discussed above is essentially a minimization problem where we try to minimize the energy functional thereby forcing level set contour to fit around the object to be segmented. The gradient of the objective functional tends to vanish at the minimizer critical points. The Euler-Lagrangian equation for the objective functional for the level set evolution keeping c_1 and c_2 constant is given in equation 9. For a detailed reading on the background of this mathematical model, the readers are encouraged to refer to [8],[9] and [10]

$$\begin{aligned} \frac{\partial \phi}{\partial t} = & \mu \delta(\phi) \operatorname{div} \left(\frac{\nabla \phi}{|\nabla \phi|} \right) \\ & + \lambda (u_0 - c_1)^2 + \lambda (u_0 - c_2)^2 \\ & + \frac{1}{1 + |\nabla \phi|^p} \quad ; p > 1 \end{aligned} \quad (9)$$

The terms μ and λ are weight terms and can be fine-tuned and customized based on the smoothness and texture properties of the image and div represents the divergence operator.

III. RESULTS AND DISCUSSIONS

The presented water delineation technique was applied on Landsat data of various lakes with surface area ranging from 0.5 km² to 300 km² and was found to produce satisfactory results. As the satellite images are captured under heterogeneous conditions, fine tuning these parameters is extremely important for the algorithm to produce accurate delineation. Figure 4 illustrates how the segmentation output changes with respect to different values of μ and λ .

The parameter values $\mu = 0.05$ and $\lambda = 1$ were found to produce the best segmentation output. Clearly, when the μ value was 1 and above, the segmentation output was unsatisfactory and also increasing λ above 2 yielded incorrect segmentation output. To establish the robustness of the algorithm, it was applied on water bodies with varying surface areas and found to produce satisfactory outputs. The water bodies chosen for the study are given in Table II and the delineation output are given in Figure 5, 6 and 7.

TABLE II: Waterbodies under study

| Lake | Location | Surface Area |
|----------------|------------------|-----------------------|
| Ulsoor | Bangalore, India | 0.5 km ² |
| Bellandur lake | Bangalore, India | 3.61km ² |
| Puzhal | Chennai, India | 18.21 km ² |
| Abjata | Ethiopia | 205 km ² |
| Dianchi | China | 298 km ² |

The potential of the proposed approach in performing change detection studies has been investigated by applying the algorithms on multi-temporal images of water bodies. Figure 7 shows the delineation output for Puzhal lake in

India during two different years, 2018 and 2019.

Quantitative validation of delineation outputs for the water bodies under study has not been performed in this work as it requires ground truth information for the water bodies for the specific time during which the satellite image was captured. The next phase of this work is proposing an algorithm to quantify the area of the delineated water bodies which can make the validation of the algorithm easier and can also be used to quantify temporal changes happening to the water bodies. In this paper, the usefulness and the potential of a hybrid level set based water delineation algorithm has been established by testing the algorithm with various water bodies of varied surface area. The proposed algorithm was compared with various proven machine learning based methods for their execution time. Supervised classification algorithm random forest executed faster than the proposed algorithm when the number of trees were two. But in this case the delineation accuracy was very less. Similarly, the unsupervised k-means clustering executed faster with only two clusters, but the the delineation accuracy suffered. Artificial Neural Networks (ANN) showed slightly faster execution but it required extensive training as it is a supervised learning algorithm. The proposed level set algorithm is a fully unsupervised algorithm and executes faster when compared with machine learning algorithms that produce comparable results. Figure 8 and Figure 9 respectively presents the execution time taken by various machine learning algorithms and the delineation output in comparison with the proposed algorithm when applied on Bellandur lake, Bangalore, India with a surface area of 3.61 km². It is worth noting that all the supervised learning algorithms require substantial amount of time and labeled data in the training phase so that the algorithm can produce accurate results. The results of the proposed method have also been compared with that of the machine learning algorithms using Pearsons correlation coefficient, Structural Similarity Index (SSIM) and Dice Similarity Index as presented in Table III.

TABLE III: Delineation output comparison using Person's correlation co-efficient, SSIM and Dice Similarity Index

| | Correlation Co-eff | SSIM | Dice Similarity Index |
|---------------|--------------------|--------|-----------------------|
| SVM | 0.706 | 0.7262 | 0.6713 |
| ANN | 0.8328 | 0.7942 | 0.7995 |
| Decision Tree | 0.8415 | 0.8109 | 0.8317 |
| RF | 0.8415 | 0.8107 | 0.8317 |
| K-means | 0.8421 | 0.8573 | 0.8297 |

A. Comparison of the algorithm with and without the edge term

The proposed algorithm is developed from a hybrid level set formulation combining the advantages of region based and edge based techniques. We have compared the performance of the algorithm with and without the edge term to emphasize the advantage of incorporating the edge term in our formulation. The experiments proved that without the edge term, the level set tend to miss the edge of the waterbodies and evolve beyond the edges resulting in inaccurate segmentation results. Figure 10 shows the segmentation output with and without the edge term. Visual interpretation of the output



Fig. 4: (a) NIR band image of Bellandur lake, Bangalore. (b) to (j) Segmentation Output variation according to different values of μ and λ

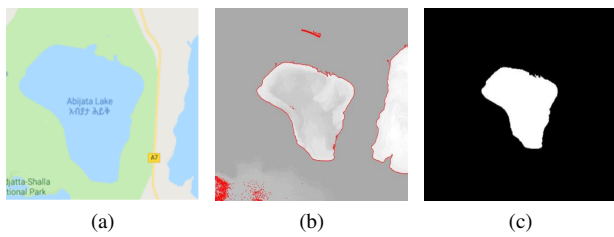


Fig. 5: Segmentation Result for Lake Abijata (a) Google maps image for visual reference. (b) Segmented image using proposed method. (c) Image after removal of unwanted regions and binarization.

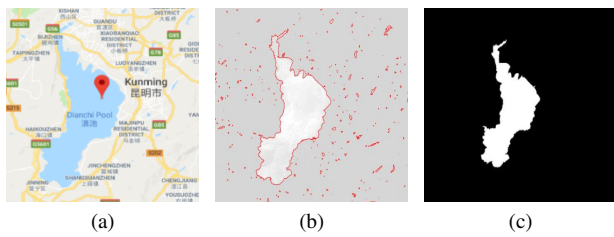


Fig. 6: Segmentation Result for Lake Dianchi (a) Google maps image for visual reference. (b) Segmented image using proposed method. (c) Image after removal of unwanted regions and binarization.

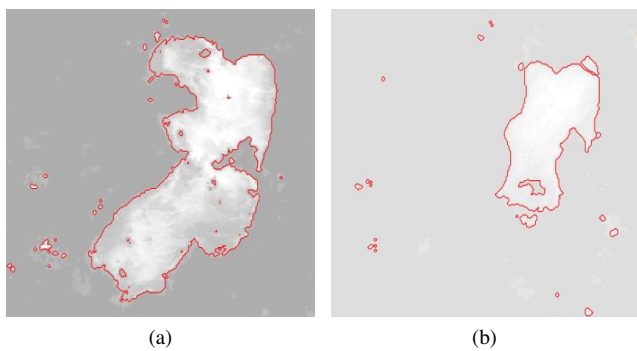


Fig. 7: Segmentation Result for Lake Puzhal (a) 2018 (b) 2019

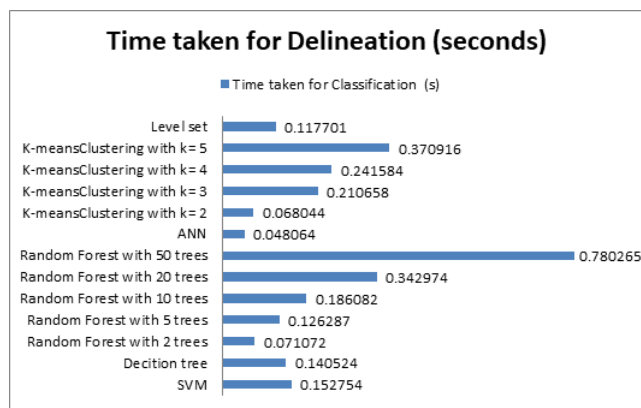


Fig. 8: Execution time comparison with machine learning based methods

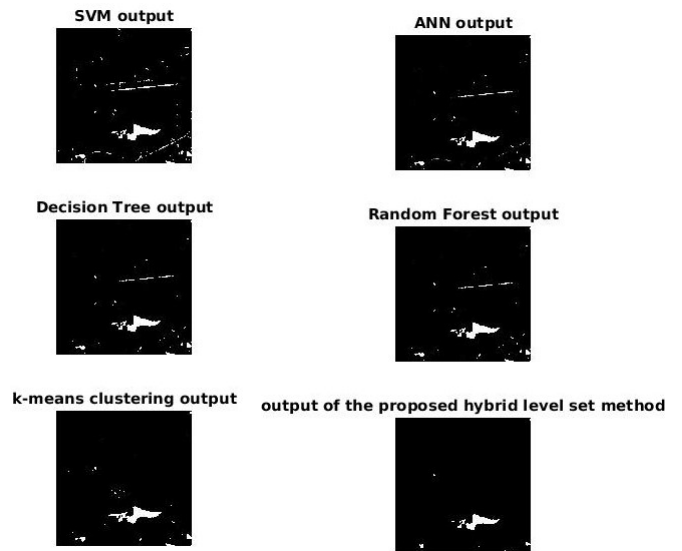


Fig. 9: Comparison of Delineation output of the proposed method with machine learning based methods

in Figure 10(a) shows that delineation without edge term performs inaccurate segmetation in the circled area of the image. Similarly in figures 10(b) and 10(c), some portion of the waterbody is not segmented properly when the edge term is omitted from the formulation. This is due to the fact that the edge term forces the level set evolution to stop at the object boundaries. We have also compared the algorithm with and without the edge term from the execution time perspective. It was found that even though the segmentation output is improved substantially with the addition of the edge term, the increase in execution time is negligible. Figure 11 presents the comparison of the respective execution times.

B. Change detection using the proposed method

This study has also explored the possibility of applying the proposed hybrid level set algorithm to multi-temporal Landsat data to perform change detection on water bodies. Change detection can be performed by collecting multi-temporal Landsat data for the study area and then applying the proposed delineation algorithm. In this work, we have collected Landsat images of Bellandur lake and Varthur lake in Bangalore from the year 1987 to 2019 and visualize the change in surface area of these water bodies over these past 30 years. Figure 12 and Figure 13 shows the temporal change in surface area over the last 30 years for Bellandur lake and Varthur lake respectively. The findings clearly show that the surface area of both water bodies has deteriorated drastically over time. This work also aims at building a data set of such images for many lakes which can later be used to build and train machine learning models to forecast the changes in water bodies.

Exponential smoothing model has been proven to be effective in lake area forecasting [21]. Exponential smoothing works by giving more weight to the recent values in the time-series data. Temporal change in surface area of water bodies happen as a result of multiple complex parameters like climate change and encroachment due to urbanization. As it

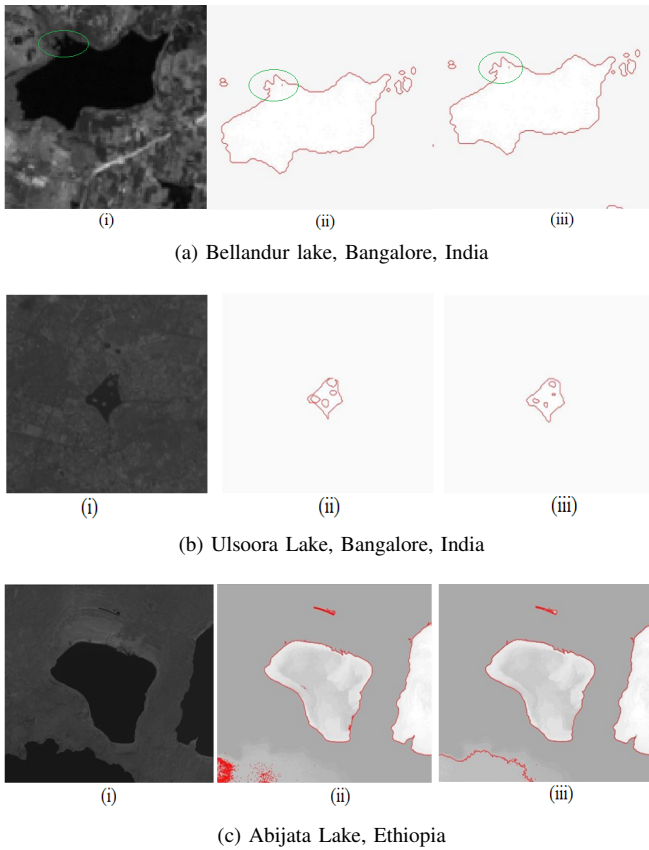


Fig. 10: Delineation output with and without the edge term (i) NIR image of the study area (ii) Delineation output without the edge term (iii) Delineation output with the edge term

is difficult to measure and quantize many of these parameters, this study does not consider any external parameters for the surface area forecast. Double exponential smoothing model utilizes two smoothing parameters to update the values at each iteration. The double exponential smoothing model representation is shown in equations 10, 11 and 12.

$$l_x = \alpha y_x + (1 - \alpha)(l_{x-1} + b_{x-1}) \quad (10)$$

$$b_x = \gamma(l_x - l_{x-1}) + (1 - \gamma)b_{x-1} \quad (11)$$

$$\hat{y}_{x+1} = l_x + b_x \quad (12)$$

l_x and b_x are the level and trend respectively at the point x in the time-series. \hat{y}_{x+1} is the fore-casted value of the surface area from the previous data which is defined in terms of level and trend. Level and trend are defined recursively in terms of their weighted values from the previous iteration. α and γ are the smoothing parameters in the double exponential smoothing model. The calculated surface area of the water body over a period of time is fed in to the forecasting model and the error functions are used to choose the best possible values for α and γ as shown in the Figures 14 and 15. Based on the mean square error plot, the smoothing model with $\alpha = 0.94$ and $\gamma = 0.5$ is chosen for surface area forecasting as presented in Figure 16

IV. CONCLUSION AND FUTURE SCOPE

A hybrid level set based water body delineation algorithm has been proposed in this work to perform change detection studies on water bodies using Landsat multi-spectral images. The proposed approach employed the combination of edge based and region based level sets to account for local and global features in the input thereby improving delineation accuracy. The robustness of the proposed algorithm has been established by applying it to delineate water bodies with surface areas ranging from 0.5 km² to 298 km². It was also established that the algorithm can be used for change detection studies by applying the algorithm to multi-temporal data. Quantitative validation of the delineation outputs was not performed due to the lack of ground truth data for the selected water bodies during the selected time frame. However, the results of the proposed method was compared with that of proven machine learning algorithms in terms of execution speed and output correlation. Once the algorithm to quantify the surface area of the water bodies is developed, validation could be performed quantitatively.

The immediate future scope for the presented method would be to propose a procedure to quantify the surface area of the delineated water bodies so that quantitative validation can be performed. This quantification algorithm in combination with the delineation algorithm could be used to develop a fully automated, fast and robust change detection and quantification system for surface water bodies. As water continues to become a scarce resource, such a system could be vital for the authorities to devise strategies to conserve our precious water bodies.

ACKNOWLEDGMENT

The School of Engineering and Technology, CHRIST (Deemed to be University) is thanked for supporting us with the requisite infrastructure and resources for this study. The United States Geological Survey (USGS) provided the satellite images for this research, which we gratefully acknowledge. We also appreciate the reviewers' insightful comments, which helped us strengthen our work.

REFERENCES

- [1] Hahmann, Thomas, and Birgit Wessel. "Surface water body detection in high-resolution TerraSAR-X data using active contour models." 8th European Conference on Synthetic Aperture Radar. VDE, pp. 1-4, 2010.
- [2] Dandawate, Y. H., and Sneha Kinlekar. "Rivers and coastlines detection in multispectral satellite images using level set method and modified Chan Vese algorithm." 2013 2nd International Conference on Advanced Computing, Networking and Security. IEEE, pp. 41-46, 2013.
- [3] Pan, Jun, and Mi Wang. "Improved seeded region growing for detection of water bodies in aerial images." *Geo-spatial Information Science*. Vol. 19, No. 1, pp. 1-8, 2016.
- [4] Xu, Chuan, Haigang Sui, and Feng Xu. "Land surface water mapping using multi-scale level sets and a visual saliency model from SAR images." *ISPRS International Journal of Geo-Information*, Vol. 5, No. 5, pp. 58, 2016.
- [5] Meng, Qingxia, et al. "Factorization-Based Active Contour for Water-Land SAR Image Segmentation via the Fusion of Features." *IEEE Access* 7, pp. 40347-40358, 2019.
- [6] Zhang, Xiaokang, et al. "Level set incorporated with an improved MRF model for unsupervised change detection for satellite images." *European Journal of Remote Sensing*, Vol. 50, No. 1, pp. 202-210, 2017.
- [7] Zhang, Mei-mei, Fang Chen, and Bang-sen Tian. "An automated method for glacial lake mapping in High Mountain Asia using Landsat 8 imagery." *Journal of Mountain Science*, Vol. 15, No. 1, pp. 13-24, 2018.

Execution Time Comparison of the Levelset algorithm with and without edge term

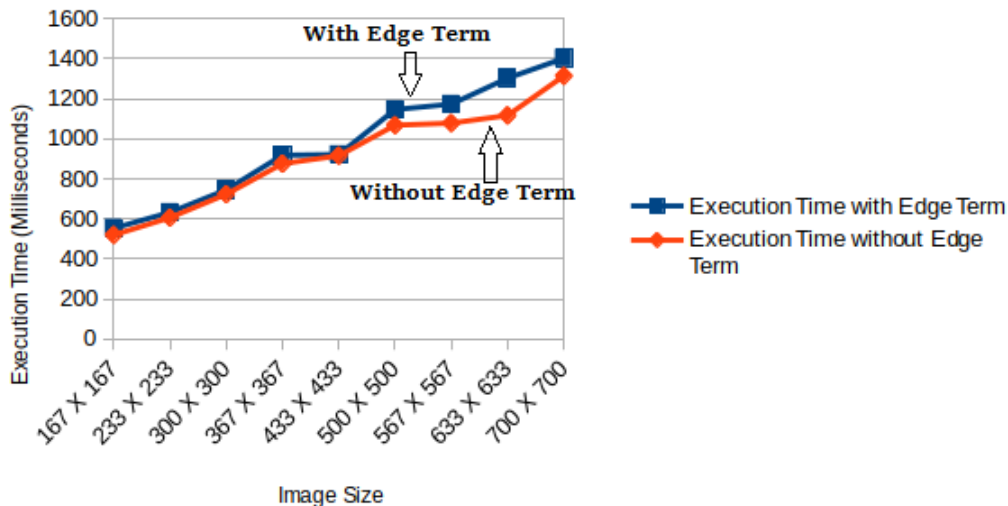


Fig. 11: Execution time comparison for the algorithm with and without the edge term

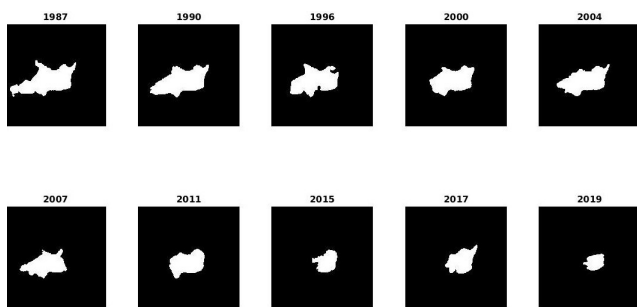


Fig. 12: Change visualization for Bellandur lake, Bangalore, India over the past 30 years using the proposed method

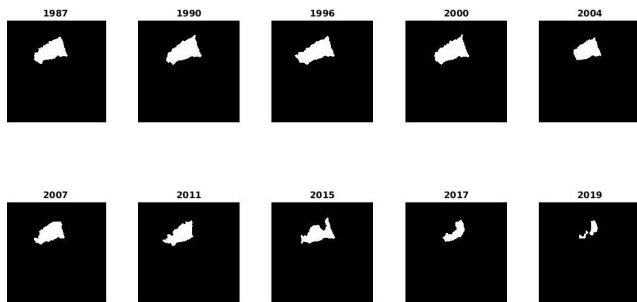


Fig. 13: Change visualization for Varthur lake, Bangalore, India over the past 30 years using the proposed method

International Conference on Pattern Recognition and Image Analysis (IPRIA). IEEE, 2017.

[14] Modava, Mohammad, and Gholamreza Akbarizadeh. "Coastline extraction from SAR images using spatial fuzzy clustering and the active contour method." *International journal of remote sensing*, Vol. 38, No. 2, pp. 355-370, 2017.

[15] Modava, Mohammad, Gholamreza Akbarizadeh, and Mohammad Soroosh. "Integration of spectral histogram and level set for coastline detection in SAR images." *IEEE Transactions on Aerospace and Electronic Systems*, Vol. 55, No. 2, pp. 810-819, 2018.

[16] Xu, H. "Modification of Normalised Difference Water Index (NDWI) to Enhance Open Water Features in Remotely Sensed Imagery." *International Journal of Remote Sensing*, Vol. 27, No. 14, pp. 3025-3033, 2006.

[17] Kass, M., Witkin, A. and Terzopoulos, D. Snakes: Active contour models. *Int J Comput Vision*, Vol. 1, pp. 321-331, 1988.

[18] Osher S., Sethian J.A., "Fronts Propagating with Curvature-Dependent Speed: Algorithms Based on Hamilton-Jacobi Formulations", *Journal of Computational Physics*, Vol. 79, No. 1, pp. 12-49, 1988.

[19] Jayadevappa, D., S. Srinivas Kumar, and D. S. Murty. "A New Deformable Model Based on Level Sets for Medical Image Segmentation." *IAENG International Journal of Computer Science*, Vol. 36, No. 3, pp. 199-207, 2009.

[20] Zhang, Kaihua, et al. "Active contours with selective local or global segmentation: a new formulation and level set method." *Image and Vision computing* 28.4 (2010): 668-676.

[21] Duan, Gonghao, and Ruiqing Niu. "Lake area analysis using exponential smoothing model and long time-series landsat images in Wuhan, China." *Sustainability*, Vol. 10, No. 1, pp. 149, 2018.

[8] Bresson, Xavier, et al. "Fast global minimization of the active contour/snake model." *Journal of Mathematical Imaging and vision*, Vol. 28, No. 2, pp. 151-167, 2007.

[9] Bresson, Xavier. "A short guide on a fast global minimization algorithm for active contour models." *Energy*, pp. 1-19, 2009.

[10] Chan, Tony F., and Luminita A. Vese. "Active contours without edges." *IEEE Transactions on image processing*, Vol. 10, No. 2, pp. 266-277, 2001.

[11] Barsi, Julia A. et al. The Spectral Response of the Landsat-8 Operational Land Imager. *Remote Sensing*, Vol. 6, pp. 10232-10251, 2014.

[12] Tv, Bijeeesh, and Narasimhamurthy Kn. "A Comparative Study of Spectral Indices for Surface Water Delineation Using Landsat 8 Images." *2019 International Conference on Data Science and Communication (IconDSC)*. IEEE, 2019.

[13] Modava, Mohammad, and Gholamreza Akbarizadeh. "A level set based method for coastline detection of SAR images." *2017 3rd*

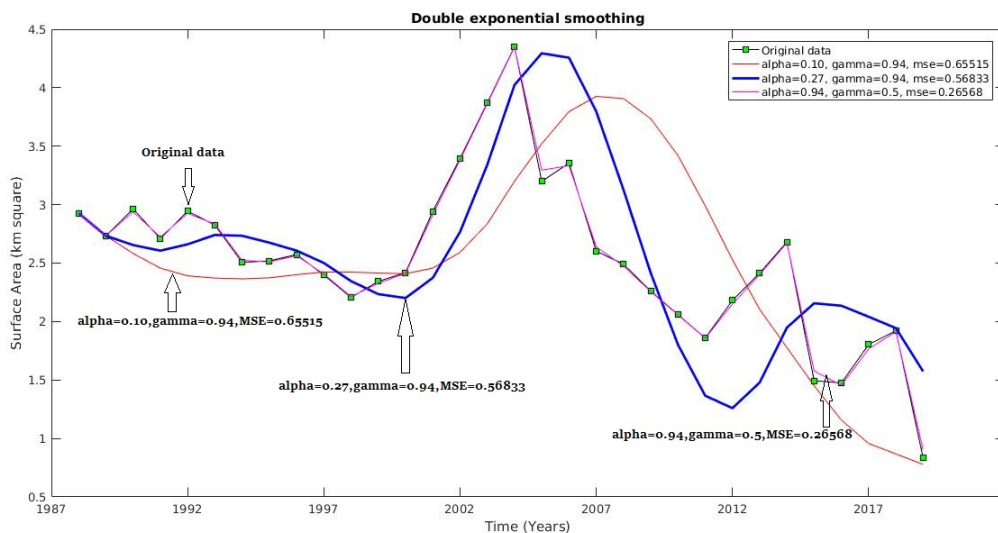


Fig. 14: Double Exponential Smoothing on Bellandur lake surface area with different values of α and γ

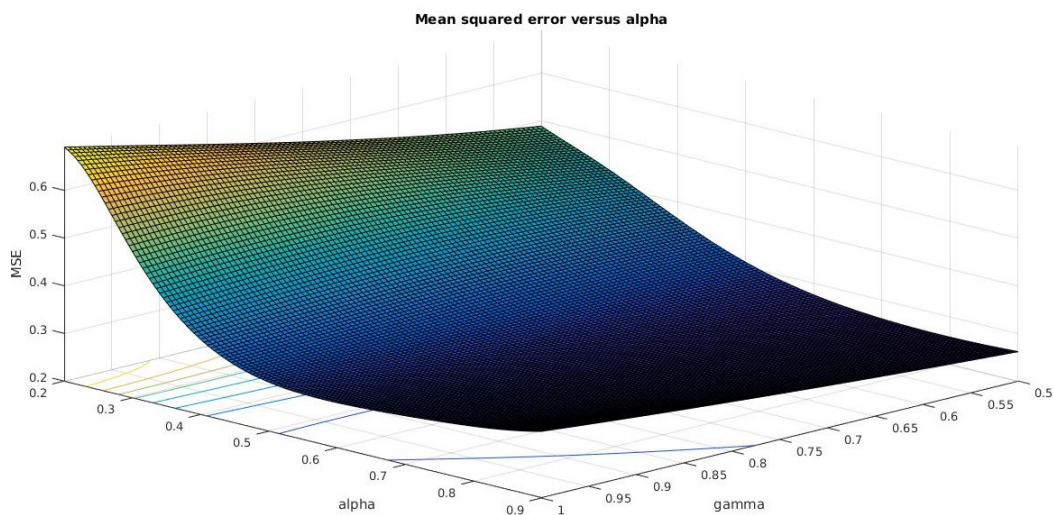


Fig. 15: Mean square error against α and γ

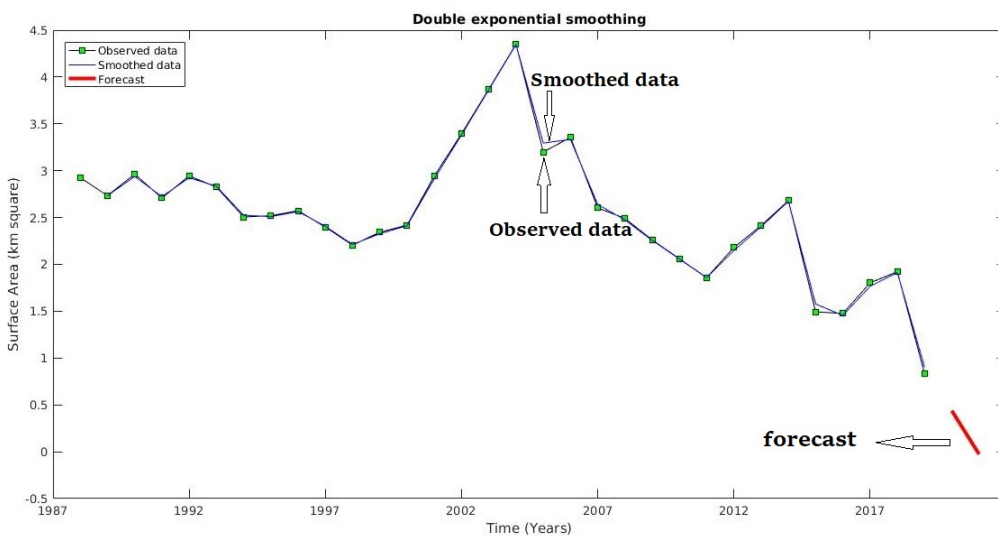


Fig. 16: Surface area forecast using Double Exponential Smoothing with $\alpha = 0.94$ and $\gamma = 0.5$